Visualization Study of Detonation Initiations Behind Reflected Shock Waves Using a High Speed Video Camera

Hiroki Yamashita[1], Jiro Kasahara[1], Akiko Matsuo[2]
[1]Department of Engimeering Mechanics and Energy, University of Tsukuba
1-1-1 Tennodai, Tsukuba, Ibaraki, 305-8573, Japan
[2]Department of Mechanics Engineering, Keio University
3-14-1 Hiyoshi, Kohoku-ku, Yokohama, 223-8522, Japan

1 Introduction

This paper is intended as an investigation of detonation initiation behind reflected shock waves, and we observed transition from a flame kernel to a detonation using a high speed video camera. Over the past 50 years, several studies have been made on the auto-ignition behind reflected shock and it has been recognized that the ignition pattern depends on the temperature[1]. These studies showed relation between induction time and temperature behind reflected shock [2,3,4]. However there were few papers which were written about detonation initiation with photograph[1]. And also behind reflected shock, boundary layer developed drastically[5]. The experiments mentioned above were conducted by dilute combustible gas with monatomic molecule gas (Argon, Krypton etc.) to reduce the influence of bounary layer. Then few papers discuss boundary layer influence on auto-ignition behind reflected shock. In order to observe the boundary layer influence on auto-ignition, stoichiometric acessylene-oxygen mixture was chosen as a combustible gas in the present study. The purpose of this study is to examine the initiation process of detonation, then deflagration to detonation transition (DDT) behind reflected shock, which has branched structure interfered with boundary layer, were observed by high speed camera and schlieren optics method.

2 Experimental setup

A shock tube was employed to this study. The shock tube is consisted of 1.4 m high- pressure section and 2.3 m low-pressure section. These sections were divided by 25 μm diaphragm, when gases were filled up. An actuator which drives needle was employed to break the diaphragm and when needle breakes the diaphragm, shock tube starts. The cross-section of the shock tube was $50 \times 50\,\mathrm{mm}$ square. First, we used helium gas and dry air, for calibration experiment, as a driver gas and a driven gas respectively. Next, dry air was replaced with combustible mixture. A stoichometric acethylen-oxgen mixture was chosen as a combustible mixture. A reflecting plate was set in the vicinity of the end of low-pressure section. Side wall around this, was replaced by glass window to visualize the phenomen. A schematic of visualization unit is illustrated in Figure 1. Schlieren method was employed for visualization using a high-speed video camera (Hyper Vision HPV-1, Shimadzu Corporation). Six pressure gauges were mounted on the shock tube. Four out of six pressure gauges were placed around the visualizetion section, as shown in Figure 1, and other two were placed 550mm, 1050mm upstream from x_3, respectively. The coordinate system was defined as shown in Figure 1 (ii).

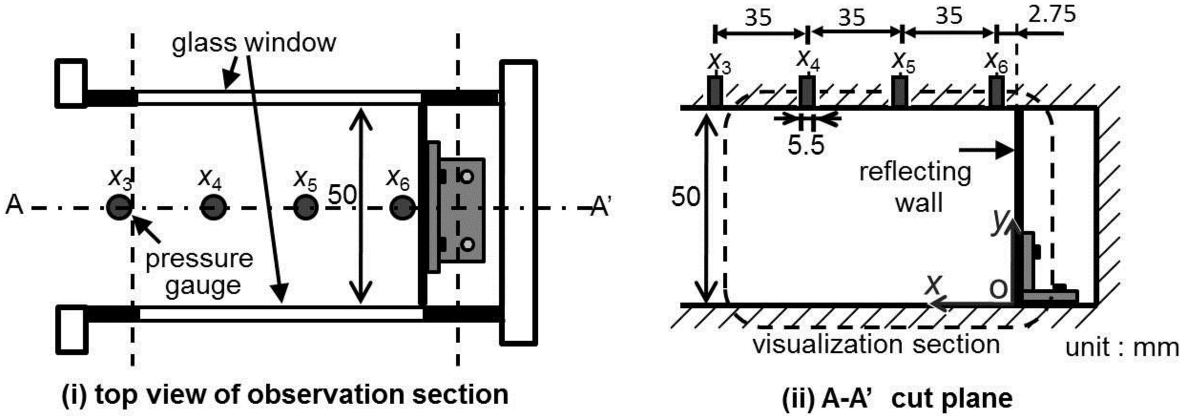

Figure 1. Schematic of visualization unit

3 Results and Discussion

3.1 Calibration of shock tube

Calibration was conducted to confirm successful shock tube operations. Helium gas, and dry air was chosen as a driver gas, and driven gas respectively. Here, each characteristic pressure values are defined as below. Initial fill pressure is p_1, time-averaged pressure during 100 μs from pressure rise of incident shock wave, is p_2, time-averaged pressure during 500 μs from pressure rise of reflected shock is p_3. Figure 2 show the comparison between experimental and theoretical p_2/p_1, p_3/p_1. Dashed lines on the Figure 2 are theoretical pressure ratio with adiabatic assumption. Here M_{si} means Mach number of incident shock. Behind reflected shock, experimental value is a little higher than theoretical value. However error bar, which is considered as measurement and analytical systematic error, contains the theoretical value. Therefore it is confirmed that shock tube was working correctly. In what follows, Rankine-Hugoniot equations with assumption based on a perfect gas, was applied to calculate pressure and temperature behind reflected shock.

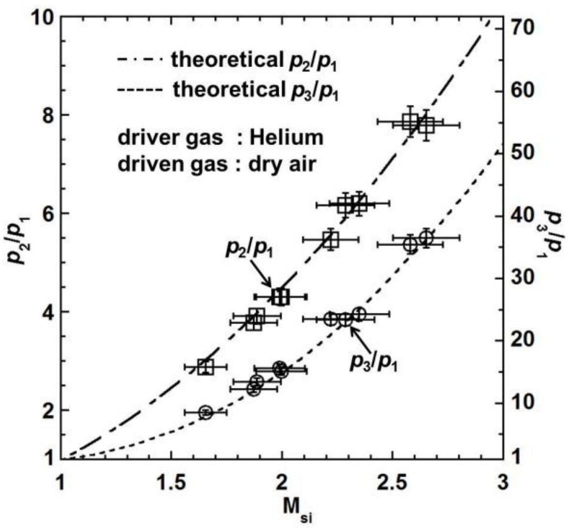

Figure 2. Pressure ratio comparison

3.2 Experimental results

In the present study, when shock wave propagated in combustible gas, we observed three cases classified as below.

(i) When Mach number of incident shock was sufficiently high, the combustible gas was ignited behind incident shock, and transited to detonation before incident shock was reflected by the reflecting plate.

(ii) When Mach number of incident shock was medium, auto-ignition occurred and transited to detonation behind reflected shock after incident shock was reflected by the reflecting plate.

(iii) When Mach number of incident shock was sufficiently low, reflected shock propagated in the combustible gas after the reflection without ignition of combustible gas.

As phenomenon (i) - (iii) mentioned above, Figure 3 shows classification of phenomenon based on the each experimental condition. In this experiment, when initial condition was around $p_1 = 5$ kPa, $\mathrm{M_{si}} = 2.7$, flame kernel occurs and transit to detonation behind reflected shock. In Figure 4, temperature (T_3) and pressure (p_3) behind reflected shock were plotted in a similar way. Here, T_3, p_3 was calculated using Rankine-Hugoniot equations. As the Figure 4 indicates, when condition was around $T_3 = 1040$ K, $p_3 = 210$ kPa, combustible gas was ignited behind reflected shock. We will now examine the phenomenon (ii) more closely in what follows.

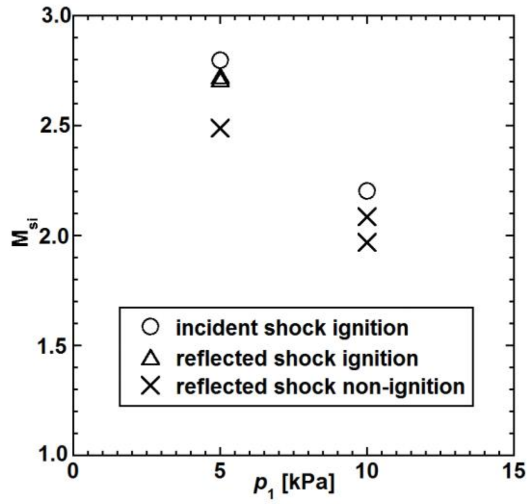

Figure 3. Classification of phenomenon based on each experimental condition

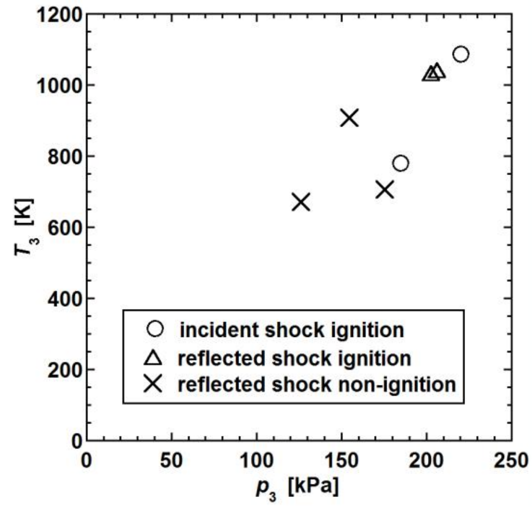

Figure 4. Classification of phenomenon based on T_3 and p_3

Visualization results, phenomenon (ii), are shown in Figure 5. In those pictures, reflected shock propagated from right to left. As it can be observed from pictures, auto-ignition occured and transited to detonation behind reflected shock. Initial condition is $p_1 = 5$ kPa, $T_1 = 295$ K, $M_{si} = 2.74$. Here, we defined the time, when incident shock reflected, is $t = 0$ μs. 1st flame kernel (1st ignition point) was observed at lower right of $t = 124$ μs in the picture. In $t = 128$ μs picture, 2nd flame kernel (2nd ignition point) was occurred. In $t = 132$ μs picture, 3rd flame kernel was came out around first flame kernel and 4th flame kernel occurred around a upper right corner. It should be emphasized that the cross-section of visualization section is 50×50 mm square. Accordingly, we have to pay attention to the depth and each flame kernel developed as 3- dimensional wave. Also, we did not observe flame kernel in the vicinity of center on glass window therefore each flame kernel was occured aound corner which is framed by glass window and top or bottom surface. From overlap region of flame kernel or detonation wave, We can estimate the ignition point. 1st and 4th flame kernel were occured at near side, 2nd and 3rd flame kernel was occured at far side. In particular, in $t = 144$μs picture, although around wave front accompanies the self-emission, center of this is still deflagration. It indicated the fact 1st flame kernel was in front of the detonation wave which transited from 2nd flame kernel. Thus, after 4μs ($t = 148$ μs), 1st flame kernel transited to detonation. These detonation wave developed with 3-dimensional-propagation and interacted each other. Eventually, detonation wave propagated from right to left in those pictures. This serise of this phenomenon is similar to mild ignition[1] which Vermeer et al. described, in terms of ignition characteristic. In the paper[1] (Vermeer et al.), ignition points were located on reflecting plate. However, in our results, ignition points were located at a point distant from reflecting plate. As a reason, while Vermeer et al. used stoichiometric *n*-heptane-oxygen mixture diluted with 70% argon to reduce interference of boundary layer, as a combustible mixture, we used a stoichiometric acethylen-oxgen mixture to observed auto-ignition behind reflected shock which has branched structure interfered with boundary layer. Therefore it is possible that the branched strucuture of reflected shock influences the ignition points of combustible gas.

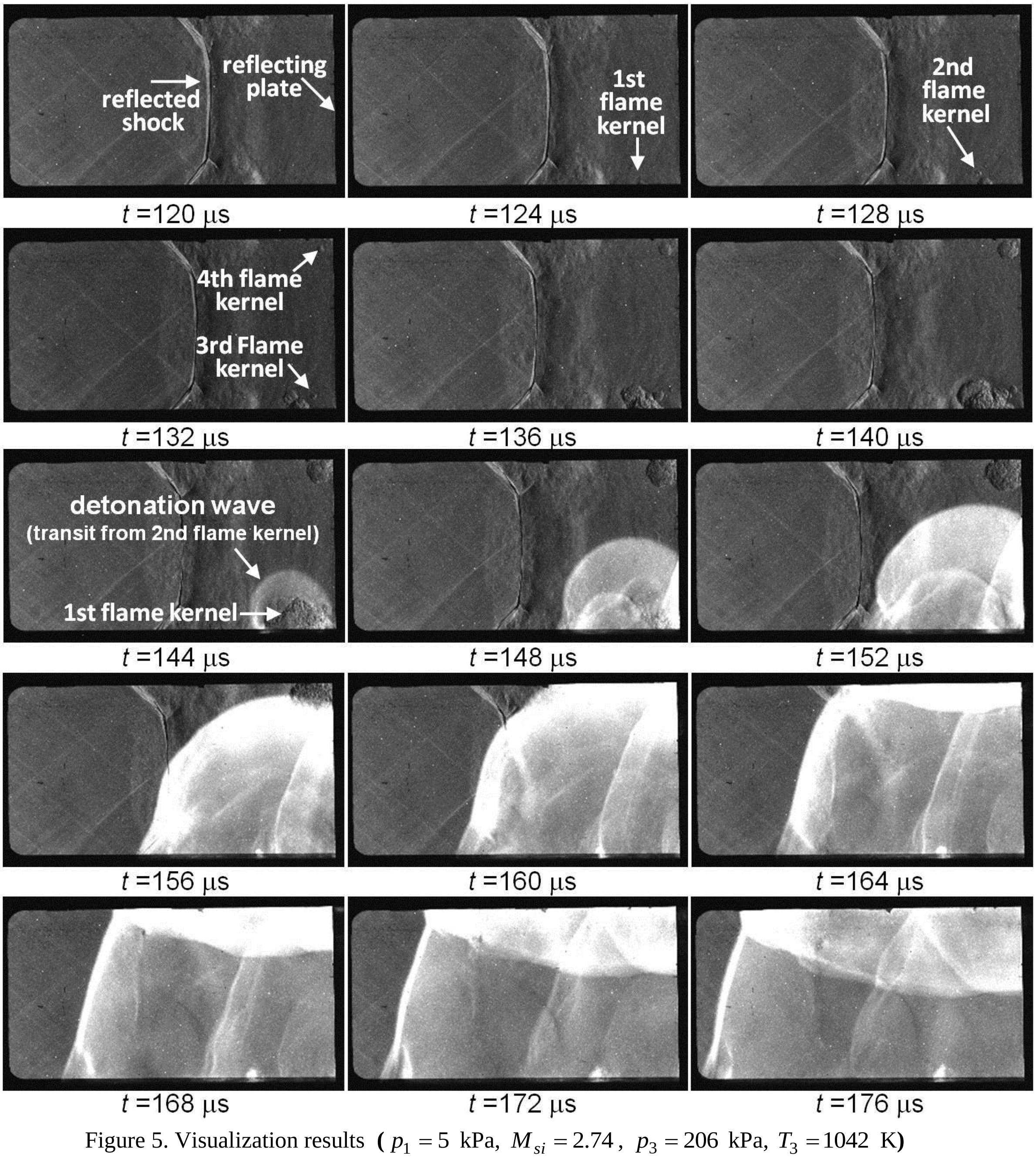

Figure 5. Visualization results **(** $p_1 = 5$ kPa, $M_{si} = 2.74$, $p_3 = 206$ kPa, $T_3 = 1042$ K**)**

Figure 6 shows the comparison between location of ignition points and the triple point trajectory of reflected shock which has branched structure. The definition of the coordinate is shown in Figure 1 (ii). In the diagram, only 1st to 4th ignition points were illustrated (Figure 5, $t = 124 \rightarrow 132$ μs). We can see the branched structure of reflected shock grew as the reflected shock propagated. The cause of branched structure development is the interference between reflected shock and boundary layer. In the present study, each flame kernel occurred in the vicinity of triple point trajectory.

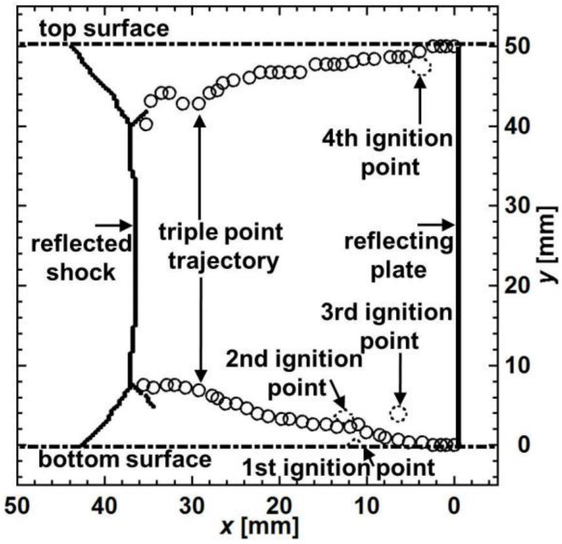

Figure 6. Location of ignition point and triple point trajectory

Figure 7 shows the time variation of 2nd flame kernel, which is scanned from schlieren results (Figure 5, $t = 140 \rightarrow 152$ μs). The definition of the coordinate is same as Figure 6. Figure 8 compares time-average velocity which are calculated from $0°$ to $135°$ by each $15°$ and CJ-velocity. These results indicated two events. First, flame kernel transited to detonation at time from $t = 140$ to $t = 144$. Second, if the detonation propagated spherically, we predicted that the velocity of detonation front was lower than CJ-velocity, because it needed a lot of power. However detonation propagated spherically with approximately CJ-velocity after $t = 144$ μs. It might be for this reason why detonation can propagate as shown Figure7, the region behind reflected shock is high-energy area as shown Figure 4 ($p_3 = 206$ kPa, $T_3 = 1042$ K).

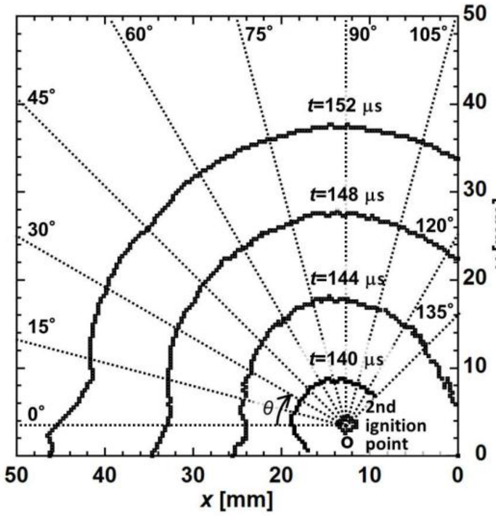

Figure 7. The time variation of 2nd flame kernel (time from t=140 to t=152)

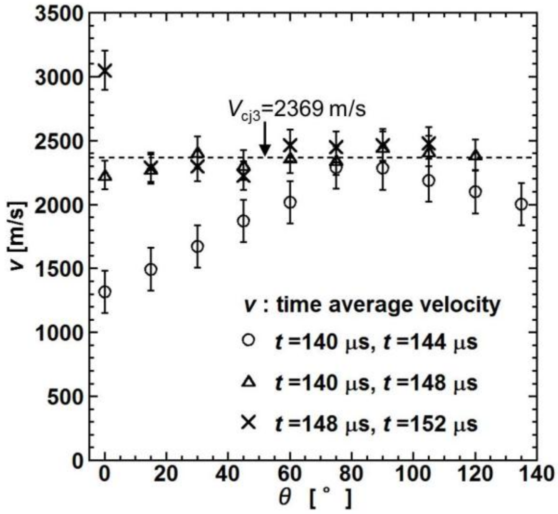

Figure 8. Distribution of wave velocity

4 Conclusions

(1) Using the shock tube and high-speed video camera, auto-ignition and transition to detonation behind reflected shock was visualized.

(2) It was inferred from Figure 6 ignition points located in the vicinity of triple point trajectory behind branching reflected shock.

(3) After flame kernel transited to detonation behind reflected shock, it propagated spherically around the corner with approximate CJ-speed. (Figure 7, 8)

References

[1] Vermeer, D.J., Meyer, J.W., Oppenheim, A.K. (1972). Auto-Ignition of Hydrocarbons behind Reflected Shock Waves. Combustion and Flame. 18: 327-336.

[2] Brown,C.J., Tomas,G.O. (2000). Experimental studies of ignition and transition to detonation by reflection and diffraction of shock waves. Shock Waves Vol. 10:23-32.

[3] Penyazkov OG et al. (2005). Autoignition of propane-air mixtures behind reflected shock waves. Proc. Combust. Inst. 30: 1941.

[4] Strehlow, R, A., Cohen, A., (1962). Initiation of Detonation. The physics of fluids.Vol. 5:97-101

[5] Mark, H. (1957). The Interaction of Reflected Shock Wave with the Boundary Layer in a Shock Tube. National Advisory Committee For Aeronautics: Technical.Memorandum 148